



Analysis of the downscaled CMCC-CM projections performed with the NMMB model

Vladimir Djurdjević and Aleksandra Kržič

**A structured network for integration of climate knowledge into policy
and territorial planning**

DELIVERABLE INFORMATION	
WP:	WP3 Mapping and Harmonising Data & Downscaling
Activity:	3.4 Development of downscaling scenarios
WP Leader:	RHMSS
Activity leader:	RHMSS and CMCC
Participating partners:	RHMSS and CMCC
Authors:	Vladimir Djurdjević, Aleksandra Kržič
E-mail:	aleksandra.krzic@hidmet.gov.rs vdj@ff.bg.ac.rs

Content

1. Introduction.....	3
2. The regional climate model NMMB	4
3. Downscaling of the period 1971-2000	5
4. Downscaling of the period 2011-2100 for RCP8.5 climate change scenario	7
4.1 Temperature change in the period 2021-2050	7
4.2 Temperature change in the period 2071-2100	7
4.3 Precipitation change in the period 2021-2050	9
4.4 Precipitation change in the period 2071-2100	9
5. Observed and expected changes of climate over Serbia	11
6. Conclusions.....	12
7. References	13

List of figures

Figure 1.1 Model domain on 8 km resolution (purple).	3
Figure 3.1 Average annual mean temperature (°C) for period 1971-2000:	5
Figure 3.2 Average annual precipitation accumulations (mm/year) for the period 1971-2000: a) NMMB, b) CARPATCLIM data set.	6
Figure 3.3 Average annual cycle for the period 1971-2000 over Serbia for NMMB and observations from national meteorological station network:	6
Figure 4.1 Maps of temperature anomalies (°C) for the periods 2021–2050 and 2071–2100 with respect to 1971–2000. Seasonal: December-January-February (DJF), March-April-May (MAM), Jun-July-August (JJA) and September-October-November (SON) and annual changes are presented from left to right.	8
Figure 4.2 Maps of precipitation change (%) for the periods 2021–2050 and 2071–2100 with respect to 1971–2000. Seasonal: December-January-February (DJF), March-April-May (MAM), Jun-July-August (JJA) and September-October-November (SON) and annual changes are presented from left to right.	10
Figure 5.1 Index example from the document.	11

1. Introduction

One of the tasks of WP3 Mapping and Harmonizing Data & Downscaling is to develop downscaling scenarios. We have already performed simulation of the present climate and verified regional model performance under so-called perfect boundary settings. The verification and capability of NMMB regional climate model to simulate present climate is shown in the report “Analysis of the downscaled ERA40 reanalysis performed with the NMMB model” (Djurdjevic and Krzic, 2013).

In this report, we have presented projections of NMMB regional climate model. Outputs from the global CMCC-CM model (Scoccimarro et al., 2011) are used as boundary conditions. Simulation is done for the period 1971-2100 and RCP8.5 climate change scenario. High-resolution simulation (8 km resolution) is performed on the smaller domain (part of the Balkan peninsula) covering four pilot areas – Covasna and Caracal county in Romania and Budapest and Veszprem in Hungary (Figure 1.1 purple).

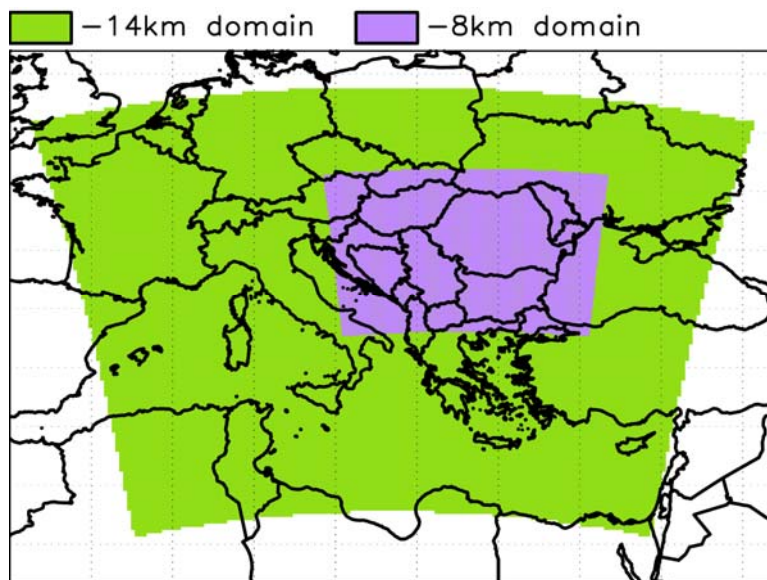


Figure 1.1 Model domain on 8 km resolution (purple).

2. The regional climate model NMMB

In recent years, the unified Non-hydrostatic Multi-scale Model (NMMB) developed at NCEP (Janjic and Gall, 2012; Janjic et al., 2011, 2013), has been used for a number of operational and research applications in Republic Hydrometeorological Service of Serbia (Djurdjevic et al., 2013). The NMMB can be run both as a global and as a regional model. The global version is run on the regular latitude-longitude grid while the regional version uses rotated latitude-longitude grid. In addition, there is a possibility to run model in a global setup with several on-line nested regional domains, which can be stationary or moving depending on user choice.

The main characteristics of the model dynamical core are that horizontal differencing preserves many important properties of differential operators and conserves a variety of basic and derived quantities including energy and enstrophy (Janjic and Gall, 2012). Model also includes the novel implementation of the nonhydrostatic dynamics (e.g. Janjic et al., 2001). Vertical coordinate in model is sigma p-hybrid coordinate.

For grid-scale convection parameterization, Betts-Miller-Janjic scheme (BMJ) is implemented (Betts, 1986; Betts and Miller, 1986; Janjic, 1994) and for turbulence model use Mellor-Yamada-Janjic (MYJ) turbulence closure sub-model (Mellor and Yamada, 1974; Mellor and Yamada, 1982; Janjic, 1990). For radiation user can choose between two radiation schemes, rapid radiative transfer model (RRTM) (Mlawer et al., 1997) and Geophysical Fluid Dynamics Laboratory (GFDL) radiation model (Fels and Schwarzkopf, 1975; Lacis and Hansen, 1974). Also two land surface packages are available, NOAH land surface model (Ek et al., 2003) and Land Ice Seas Surface model (LISS) (Vukovic et al., 2010). Finally, for cloud microphysics two packages are available as well, cloud microphysics scheme of Ferrier et al. (2002) and microphysics following Zhao and Carr (1997).

The regional version of the NMMB recently replaced the WRF NMM as the main NCEP's operational short range forecasting model for North America (NAM).

3. Downscaling of the period 1971-2000

Period 1971-2000 was chosen as a reference period integration. Verification of downscaling results for this time period is done using E-OBS data set (Haylock et al., 2008), CARPATCLIM data set (Spinoni et al., 2014) and national meteorological stations network from Serbia (Djurdjevic and Krzic, 2013).

Spatial distributions of the average annual mean temperature from NMMB model integration and from E-OBS data set are presented in Figure 3.1. It can be seen that model has negative bias ranging between 2 and 3°C over the whole domain. The bias is lower on mountain peaks in comparison to low land parts (e.g. Pannonia flat). Figure 3.3 depicts annual cycle of monthly mean temperatures from NMMB reference period integration and from Serbian national meteorological observations. The average is calculated over the territory of Serbia. Annual cycle is well resembled but negative bias is present throughout the entire year for all months. The bias is lower for summer months in comparison to winter months.

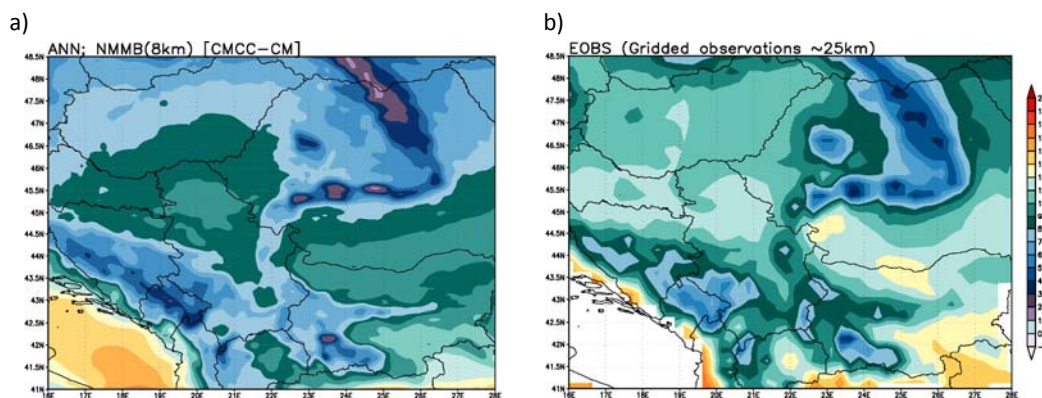


**Figure 3.1 Average annual mean temperature (°C) for period 1971-2000:
a) NMMB, b) E-OBS data set.**

Figure 3.2 presents spatial distribution of the average annual precipitation accumulations from CARPATCLIM data set together with results from NMMB model. Simulated precipitation amounts are compared with CARPATCLIM dataset and not with E-OBS as for the temperature not only because of increased resolution of grid (25 km for E-OBS and 10 km for CARPATCLIM) but meteorological station network used for construction of CARPATCLIM is much denser in comparison to network used for E-OBS. Positive bias is present in most of the area but there are also sub domains with negative bias in annual accumulations, such as central and southern part of Romania. The positive bias is specially amplified on eastern and southern peaks of Carpathian Mountains.

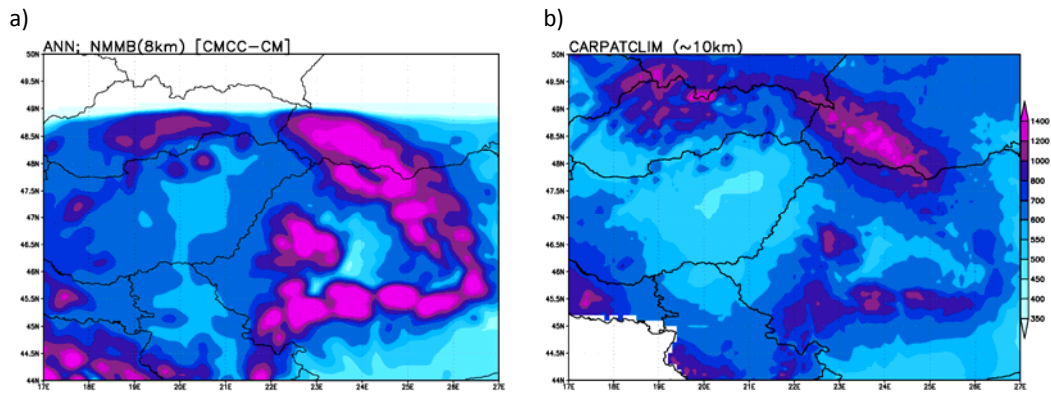


Figure 3.2 Average annual precipitation accumulations (mm/year) for the period 1971-2000: a) NMMB, b) CARPATCLIM data set.

As for Serbia, the positive precipitation bias is found for months from January to May and November and December (Figure 3.3) and negative bias was found for June, August and September. For July and October long term mean for monthly precipitation is very close to observed values with biases less than 1%. The largest positive bias is for January and the largest negative bias is for August. Similar bias distribution can be found in COSMO-CLM downscaling of the same global model simulations for domain covering Italy and western Balkan (Montesarchio et al., 2013).

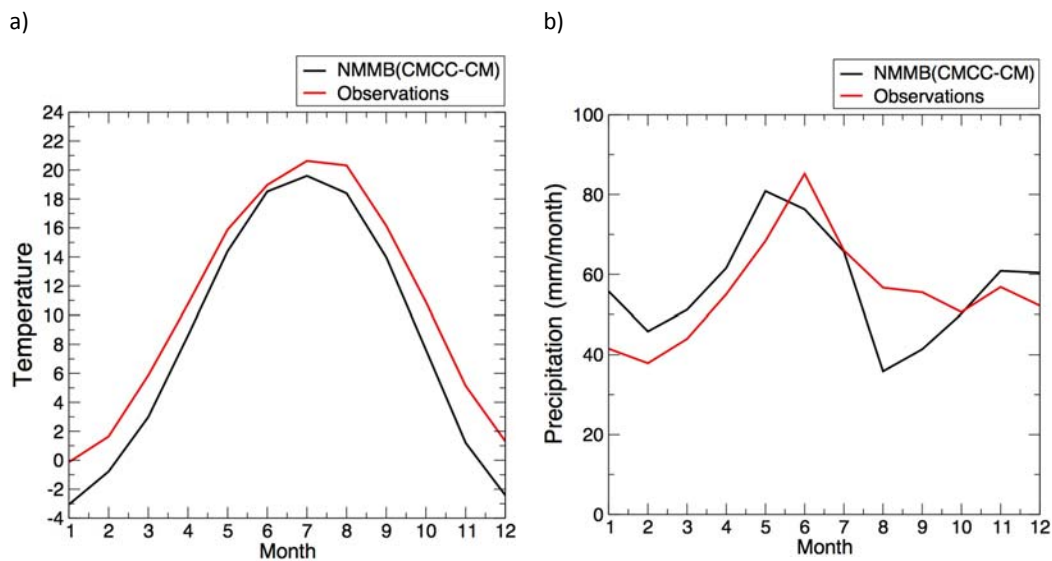


Figure 3.3 Average annual cycle for the period 1971-2000 over Serbia for NMMB and observations from national meteorological station network: a) temperature (°C), b) precipitation (mm/month).

4. Downscaling of the period 2011-2100 for RCP8.5 climate change scenario

4.1 Temperature change in the period 2021-2050

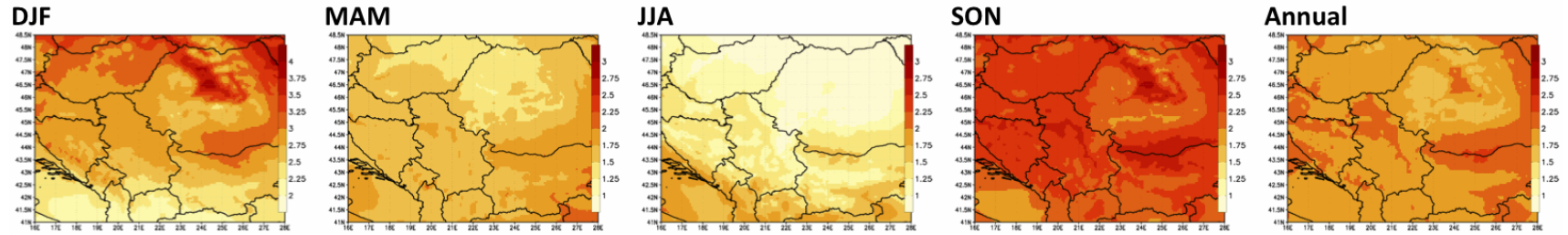
Figure 4.1 shows anomaly maps of surface air temperature ($^{\circ}\text{C}$; 2021–2050 with respect to 1971–2000 for the RCP8.5 scenario) from NMMB model downscaling of CMCC-CC GCM integration (upper panels). Changes are presented for four seasons: December-January-February (DJF), March-April-May (MAM), Jun-July-August (JJA) and September-October-November (SON) and as annual means. For DJF season temperature change ranges from 2 to 4°C with mean value of about 3°C . In comparison to other seasons, temperature increase is the highest for DJF.

For MAM, JJA and SON temperature change ranges from 1 to 3°C within domain. The highest values are for SON season with mean value of about 2.5°C . The lowest values are for JJA season, especially in northeast part of domain. In general, higher increase was found for lowland areas and river plains (Morava in Serbia, and Danube in Romania) during all seasons. On annual level temperature increase is from 2 to 2.5°C .

4.2 Temperature change in the period 2071-2100

Anomaly maps of surface air temperature ($^{\circ}\text{C}$) for the period 2071–2100 with respect to 1971–2000 for the RCP8.5 scenario are presented on lower panels in Figure 4.1. Temperature increase for the last thirty years of the 21st century in comparison to the period 2021-2050 is about 3 to 4°C higher. For DJF season temperature increase is in a range from 5 to 7°C , for JJA and SON from 4 to 6°C and the lowest increase is for MAM season - from 4 to 5°C . Similarly to the period 2021-2050, higher increase was found for lowland areas and river plains. Strong gradient in temperature increase is present from northeast to southwest part of the domain during DJF and JJA seasons but with different sign. Temperature increase is highest in northeast during DJF and in southwest part during JJA. Average increase in annual mean temperature is about 5.5°C over domain.

RCP 8.5 period 2021-2050 w.r.t 1971-2000



RCP 8.5 period 2071-2100 w.r.t 1971-2000

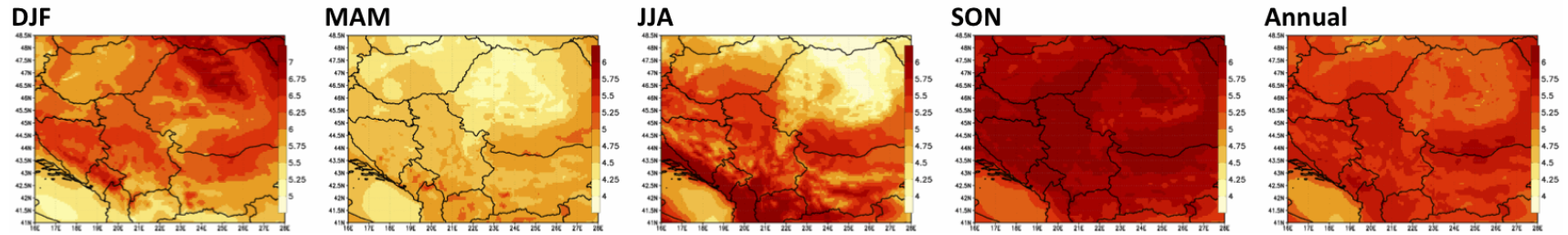


Figure 4.1 Maps of temperature anomalies (°C) for the periods 2021–2050 and 2071–2100 with respect to 1971–2000. Seasonal: December-January-February (DJF), March-April-May (MAM), Jun-July-August (JJA) and September-October-November (SON) and annual changes are presented from left to right.

4.3 Precipitation change in the period 2021-2050

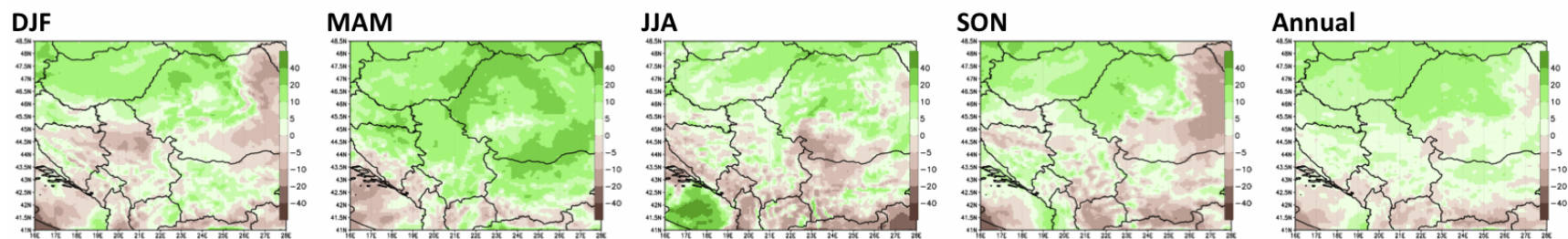
Figure 4.2 depicts maps of precipitation change (in %) for the period 2021–2050 with respect to 1971–2000 and for the RCP8.5 scenario from NMMB model downscaling of CMCC-CC GCM integration (upper panels). Similar patterns in precipitation change were found for seasons DJF, JJA and SON. Increase in precipitation amount (from 5 to 20%) was found in the northern part of the model domain while in southern part both, increase and decrease, are present. In some regions decrease of -20% can be observed. For MAM season increase in precipitation is characteristic for almost the entire observed area except over Dinaric Mountains and some areas close to southern domain boundary. Increase ranges from 5 to 20%. Spatial pattern of annual precipitation change is similar to DJF, JJA and SON seasons with values ranging from -20 to 20%.

4.4 Precipitation change in the period 2071-2100

Strong decrease in average precipitation amounts was found during summer season for the period 2071-2100 with values lower than -40% (Figure 4.2, lower panels). Most of domain has negative change, lower than -20%. Conversely, for DJF season, majority of domain has positive change with values higher than -2% but for some areas in central, eastern and southern part of domain negative change is also found. In general, positive gradient is present from south to north part of the domain.

Precipitation decrease can be observed in western and southern parts of domain during MAM and in eastern and southern parts during SON. Change in average annual amount of precipitation is negative for almost whole domain with mean value of about -10%.

RCP 8.5 period 2021-2050 w.r.t 1971-2000



RCP 8.5 period 2071-2100 w.r.t 1971-2000

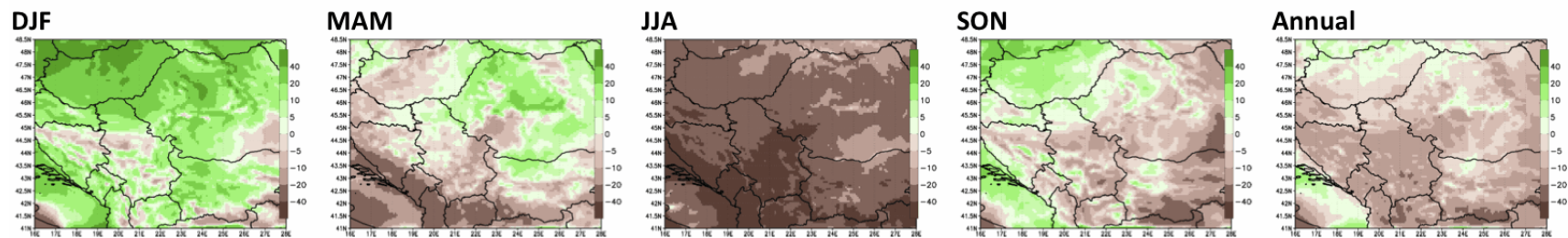


Figure 4.2 Maps of precipitation change (%) for the periods 2021–2050 and 2071–2100 with respect to 1971–2000. Seasonal: December-January-February (DJF), March-April-May (MAM), Jun-July-August (JJA) and September-October-November (SON) and annual changes are presented from left to right.

5. Observed and expected changes of climate over Serbia

In order to obtain a uniform perspective on perceived changes in weather and climate extremes, the set of 27 extreme indices is proposed by Expert Team on Climate Change Detection and Indices (ETCCDI) within the WMO. For their calculation it is necessary to have daily data of temperature (minimum and maximum) and accumulated precipitation.

In separate analysis, expected changes in climate indices for the period 2011-2040 (with respect to the period 1971-2000) are obtained using results from the NMMB model. These changes are compared with climate indices calculated from observed data from 38 meteorological stations in Serbia covering the period 1971-2000.

Prior indices calculation all observational datasets are quality controlled and homogenized. After the homogenization, observations are used for bias correction of the modeled data. All 27 indices are calculated by RCLimDex program packet and mapped using R software (kriging method).



Figure 5.1 Index example from the document.

This analysis will be published in the form of the document in Serbian language - Analysis of extreme climate indices for territory of the Republic of Serbia ("Анализа

индекса климатских екстрема за територију Републике Србије”, Davidovic et al.,2015). The document comprises:

- spatial distribution of mean values of historical indices for the period 1971-2000;
- diagrams of decadal trends of the indices and its significance per station;
- spatial distribution of departure of the mean index values calculated on the basis of the model projection for the period 2011-2040 compared with the model simulation 1971-2000;
- accompanying description of the figures.

Additional illustrations are used to highlight the importance of a given index for a particular sector of the economy (health care, agriculture and food supply, water management and hydrology) as it is defined by the Expert Team on Climate Risk and Sector-Specific Climate Indices (ET-CRSCI).

6. Conclusions

In the previous report “Analysis of the downscaled ERA40 reanalysis performed with the NMMB model” we have shown that model is capable for reproduction of observed climate. By increasing the model resolution we obtained better results especially for precipitation accumulations. Detailed analysis of daily precipitation distributions revealed that reason for this is convection permitted resolution of model, which enables better representation of summer heavy precipitation episodes.

In this paper, we presented the possible future changes in temperature and precipitation according to the downscaling results of the global CMCC-CM model. For downscaling we used NMMB regional climate model and applied RCP8.5 climate change scenario. Simulation is done for the period 1971-2100 on 8 km resolution.

For the reference period 1971-2000 model has negative temperature bias compared to temperature observations (2-3°C over the whole domain). The largest differences are over the plains. Temperature annual cycle is resembled well but negative bias is present over the whole year. Regarding precipitation, NMMB integrations generally overestimate annual precipitation especially on the mountain peaks.

For the future we examined changes in temperature and precipitation for two periods – closer future 2021-2050 and the last 30 years of the century compared to the reference period 1971-2000. There is a constant increase in temperature during the 21st century – around 2 degrees in the first period and up to 6 degrees in the period 2071-2100. In addition, in the first period there is a precipitation increase in the northern part of the domain. In the second period change is negative for almost

whole domain with mean value of about -10%. Seasonal values show that the highest temperature increase is expected for winter season up to 4 degrees in the first and up to 7 degrees in the second period, while the lowest increase is expected during summer and spring. Higher increase is over lowland areas and river plains. Larger amounts of precipitation are simulated for northern parts of the domain in all seasons for the period 2021-2050. In the second period there are two extreme seasons – summer as extremely dry with precipitation decrease of -40%, and winter as wet season with the precipitation increase of 40%.

The data provided by the NMMB model could be distributed to the ORIENTGATE partners via an FTP server set up. Access request should be addressed to Aleksandra Kržič (aleksandra.krzic@hidmet.gov.rs; CC to vdj@ff.bg.ac.rs).

7. References

Betts A.K., 1986: A new convective adjustment scheme. Part 1: Observational and theoretical basis, *Q.J.Roy.Meteorol.Soc.*, 112, 677–691, doi:10.1002/qj.49711247307

Betts A.K. and Miller M.J., 1986: A new convective adjustment scheme, Part II: Single column tests using GATE wave, BOMEX, ATEX and arctic air-mass data sets, *Q. J. Roy. Meteorol. Soc.*, 112, 693–709, doi:10.1002/qj.49711247308

Davidovic U., Krzic A., Simic G. and Milic-Petrovic B., 2015: Анализа индекса климатских екстрема за територију Републике Србије. In preparation

Djordjevic V., Janjic Z., Pejanovic G., Vasic R., Rajkovic B., Djordjevic M., Vujadinovic M., Vukovic A. and Lompar M., 2013: NCEP’s multi-scale NMMB model in the Hydrometeorological Service of Serbia: experiences and recent model developments, *EGU General Assembly, Geophysical Research Abstracts, Vol. 15, EGU2013-8217, 7-12 April 2013, Vienna*

Djordjevic V. and Kržič A., 2013: Analysis of the downscaled ERA40 reanalysis performed with the NMMB model, ORIENTGATE project report

Ek M.B., Mitchell K.E., Lin Y., Rogers E., Grunmann P., Koren V., Gayno G. and Tarpley J.D., 2003: Implementation of Noah land surface model advances in the National Centers for Environmental Prediction operational mesoscale Eta model, *J. Geophys.Res.*, 108, 8851, doi:10.1029/2002JD003296

Fels S.B. and Schwarzkopf M.D., 1975: The simplified exchange approximation - A new method for radiative transfer calculations, *J. Atmos. Sci.*, 32, 1475–1488

Ferrier B.S., Jin Y., Lin Y., Black T., Rogers E. and DiMego G., 2002: Implementation of a new grid-scale cloud and precipitation scheme in the NCEP Eta Model, in: *Proceedings of the 15th Conference on Numerical Weather Prediction*, 280–283

Haylock M.R., Hofstra N., Klein Tank A.M.G., Klok E.J., Jones P.D. and New M., 2008: A European daily high-resolution gridded dataset of surface temperature and precipitation. *J. Geophys. Res (Atmospheres)*, 113, D20119, doi:10.1029/2008JD10201

Janjic Z.I., 1990: Physical package for step-mountain, Eta coordinate model, *Mon. Weather Rev.*, 118, 1429–1443

Janjic Z.I., 1994: The Step-Mountain Eta Coordinate Model: Further Developments of the Convection, Viscous Sublayer, and Turbulence Closure Schemes, *Mon. Weather Rev.*, 122, 927–945

Janjic Z.I., Gerrity J.P.Jr, Nickovic S., 2001: An alternative approach to nonhydrostatic modelling. *Mon. Wea. Rev.*, 129, 1164–1178

Janjic Z., Janjic T. and Vasic R., 2011: A Class of conservative fourth order advection schemes and impact of enhanced formal accuracy on extended range forecasts, *Mon. Weather Rev.*, 0, null, doi:10.1175/2010MWR3448.1

Janjic Z. and Gall R.L., 2012: Scientific documentation of the NCEP nonhydrostatic multiscale model on the B grid (NMMB). Part 1 Dynamics. NCAR Technical Note NCAR/TN-489+STR, DOI: 10.5065/D6WH2MZX

Janjic Z., Djurdjevic V., Vasic R., Ferrier B. and Lin H-M., 2013: NCEP's Multi-scale Eulerian NMMB model, EGU General Assembly, Geophysical Research Abstracts, Vol. 15, EGU2013-6557, Vienna

Lacis A.A. and Hansen J.E., 1974: A parameterization for the absorption of solar radiation in the Earth's atmosphere, *J. Atmos. Sci.*, 31, 118–133

Mellor G. and Yamada T., 1974: A hierarchy of turbulence closure models for the planetary boundary layer, *J. Atmos. Sci.*, 31, 1791– 1806

Mellor G.L. and Yamada T., 1982: Development of a turbulence closure model for geophysical fluid problems, *Rev. Geophys. Space Phys.*, 20(4), 851–875

Mlawer E.J., Taubman S.J., Brown P.D., Iacono M.J. and Clough S.A., 1997: Radiative transfer for inhomogeneous atmospheres: RRTM, a validated correlated-k model for the long-wave, *J. Geophys. Res.*, 102, 16663–16682

Montesarchio M., Zollo A.L., Cavicchia L. and Mercogliano P., 2013: Analysis of the downscaled climate simulations performed with the COSMO-CLM model, including assessment of the bias, ORIENTGATE project report

Scoccimarro E., Gualdi S., Bellucci A., Sanna A., Fogli P.G., Manzini E., Vichi M., Oddo P. and Navarra A., 2011: Effects of Tropical Cyclones on Ocean Heat Transport in a High Resolution Coupled General Circulation Model. *Journal of Climate*, 24, 4368-4384

Spinoni J. and the CARPATCLIM project team (39 authors), 2004: Climate of the Carpathian Region in 1961-2010: Climatologies and Trends of Ten Variables. *Int. J. Climatol*, DOI: 10.1002/joc.4059

Vukovic A., Rajkovic B. and Janjic Z., 2010: Land Ice Sea Surface Model: Short Description and Verification, 5th International Congress on Environmental Modelling and Software, Ottawa, Ontario, Canada

Zhao QY. and Carr F.H., 1997: A prognostic cloud scheme for operational NWP models. *Mon. Wea. Rev.*, 125, 1931-1953